Supporting Calculations for NASA's IRIS Mission. I. Overview

Eugene Avrett

Harvard-Smithsonian Center for Astrophysics, 60 Garden Street, Cambridge, MA 02138

Understanding the solar chromosphere continues to be a fundamental challenge in solar and heliospheric physics. The chromosphere is the region located above the cooler photosphere where the visible spectrum originates, and below the extended much hotter corona where flares and mass ejections occur. The outward increase of temperature in the chromosphere remains essentially unexplained.

NASA's Interface Region Imaging Spectrograph (IRIS) mission, to be launched in December 2012, is devoted to the study of this interface between photosphere and corona. The objective is to trace the flow of energy and plasma through the chromosphere using high-resolution imaging and spectroscopy. In order to interpret the observations, theoretical simulations are needed. Advances are being made in computing the spectrum emitted from solar chromospheric regions based on assumed atmospheric properties such as temperature, density, flow velocity, and chemical composition, and based on theoretical simulations of atmospheric structure. Such model computations are complex because the chromosphere is optically thick and is radiation-dominated so that conditions at one location depend on the conditions at all other locations, and because there are strong radiative interactions throughout the spectrum between different atoms, ions, and molecules. Also, magnetic fields influence the structure of various regions.

IRIS will observe the spectrum in three ultraviolet wavelength bands, emitted from a variety of dark and bright features on the solar disk. These wavelength bands include emission lines which are produced in the chromosphere and which are sensitive to the physical properties of this emitting region. Computer simulations can be carried out to determine the structure of the atmosphere corresponding to observed spectra

Mg II k is a resonance line of ionized magnesium centered at the ultraviolet wavelength 2796.4 Å. It is a solar emission line because the line center intensity is emitted from regions high in the chromosphere where the temperature is much larger than in the low chromosphere where the line wings, displaced from line center, are emitted. The line opacity is maximum at line center and diminishes in the wings. This emission line is centrally reversed, with the central intensity smaller than in the near wings because of the escape of radiation in the surface layers which reduces excitation in these layers. Mg II k is only one of a group of lines to be observed and analyzed, but it is perhaps the most useful one for the study of the structure and behavior of the chromosphere.

The emission in this line varies with position on the solar disk in two ways: from feature to feature and from center to limb. The dark-to-bright features range from sunspot umbrae and penumbrae, internetwork cells and the brighter network, and from plages, faculae, and flares. Also, there are the coronal-hole regions where coronal emission is reduced, producing some changes in the chromosphere. While there are order-of-magnitude intensity differences from feature to feature,

the differences in brightness temperature and corresponding gas temperature in the chromosphere are no more than several hundred degrees, according to 1-D modeling. However, current 3-D dynamical modeling indicates much larger temperature variations, and the two approaches need to be reconciled.

The observed changes in intensity from center to limb for a given feature provide height discrimination, since a given optical depth along the line of sight toward a region close to the solar limb will be reached higher in the atmosphere than along the line to disk center.

In addition to these two ways in which the intensity varies with position on the disk, gas motions cause Doppler shifts in the line profiles. In the case of a vertical mass-conserving flow, in which velocity is inversely proportional to density, and density decreases with increasing height, lines and parts of lines that are emitted higher in the atmosphere will have greater shifts in wavelength than those emitted lower in the atmosphere. This changes the shape of a line profile.

Here we illustrate these three effects using calculated Mg II k profiles. These calculated results are roughly consistent with observations from past rocket and satellite experiments, but the past observations had much lower resolution than is expected from IRIS. The calculated profiles shown here are obtained from 1-D plane-parallel models, thus representing the emission along a given line of sight, given the atmospheric properties along that line, and assuming little influence from regions along neighboring regions having different properties. This is a reasonable approximation when features such as internetwork and network regions have horizontal dimensions much larger than their vertical extent. But some features are more localized and are influenced by radiation from neighboring regions with different properties. Atmospheric motions and variations with time also need to be taken into account. The present discussion is restricted to 1-D modeling.

a) Feature-to-feature effects. Figure 1 shows the disk-center k-line profiles calculated from six atmospheric models, corresponding to the average quiet Sun and to five brightness components: faint internetwork, mean internetwork, bright network, bright plage, and bright facula. The average quiet-Sun model is from Avrett & Loeser (2008), and the component models are from Fontenla et al. (2011). (The non-thermal broadening velocities in the Fontenla et al. models for the faint and mean internetwork and network cases are much larger than in the other cases, and we have rescaled these broadening velocities to give roughly the same peak-to-peak wavelength separation as in the other cases.) The calculated profiles are shown in color. The corresponding ones in black have been convolved with a Gaussian instrumental profile having a FWHM of 80 mÅ, representing the expected IRIS resolution. These intensities are quite sensitive to chromospheric temperature: temperature changes of only a few hundred degrees give order of magnitude intensity variations.

b) Center-to-Limb effects. Figure 2 shows the intensity profiles calculated from the average quiet Sun model for six disk positions, $\mu = 1.0$, 0.7, 0.4, 0.2, 0.1, and 0.05, where μ at a given point on the solar surface is the cosine of the angle between the solar vertical and the direction to the observer. Thus $\mu = 1$ is at disk center, and $\mu = 0.05$ corresponds to the fraction 0.9999 of the disk radius. Only the convolved profiles are shown in this figure and in the two subsequent ones.

c) Velocity effects. We now show the effects of outflows and inflows which are mass conserving in that the flow velocity is inversely proportional to the gas density. We choose vertical flow velocities V = 10, 20, and 50 km/s at the height where the total hydrogen number density nH has the value $10^{10}\mathrm{cm}^{-3}$. The temperature is 22,000 K at this height in the average quiet-Sun model. Unit optical depth in the center of the k line occurs deeper in the atmosphere where the temperature is roughly 6700 K and nH is 4.5×10^{10} in the average quiet-Sun model. Thus V = 2.2, 4.4, and 11 km/s at line-center optical depth unity in this stationary model.

The flow velocity increases with increasing height as nH decreases. Since the line center intensity originates higher in the atmosphere than the line wings, V will cause a greater Doppler shift of the line center than of the wings, thus dininishing one peak or the other. The results for outflows appear in Figure 3, and those for inflows in Figure 4.

These comparisons show how the relative intensities of the blue and red emission peaks depend on vertical flows. The k line observed from the average quiet Sun shows that the red peak intensity is roughly 0.86 times the blue peak intensity. See Staath & Lemaire (1995). This corresponds to a smaller inflow velocity than the values illustrated here. In Fig. 4, the red-to-blue peak intensity ratios are 0.77, 0.59, and 0.37. It should be pointed out that the mass-conserving flow velocities become unrealistic at very small densities where flows can diverge along diverging magnetic field lines. A better approximation may be to specify a mass-conserving flow up to a certain height in the atmosphere which then remains constant above this height. Other lines to be observed in the IRIS mission are emitted higher in the atmosphere and should help determine the flow velocity in given features. The other principal lines to be observed are Mg II h at 2803.5Å, O I 1355.6 Å, C II 1334.5 Å, 1335.7 Å, O IV 1399.8 Å, 1401.2 Å, and Si IV 1393.8 Å, 1402.8 Å.

Further calculations will be carried out to produce an extensive set of 1-D calculated profiles for all of these lines corresponding to different observed features at different disk positions with various outflows and inflows. These results should provide a useful basis for the interpretation of the IRIS observations, and for the interpretation of the more complex 3-D dynamical modeling calculations.

I thank Sean McKillop for his assistance with this work.

References

Avrett, E. H., & Loeser, R. 2008, Models of the solar chromosphere and transition region from SUMER and HRTS observations: Formation of the extreme-ultraviolet spectrum of hydrogen, carbon, and oxygen, ApJS, 175, 229

Fontenla, J. M., Harder, J., Livingston, W., Snow, M., & Woods, T. 2011, High-resolution solar spectral irradiance from extreme ultraviolet to far infrared, J. Geophys Res., 116 D20108

Staath, E. & Lemaire, P. 1995, High resolution profiles of the Mg II h and Mg II k lines, A&A, 295, 517

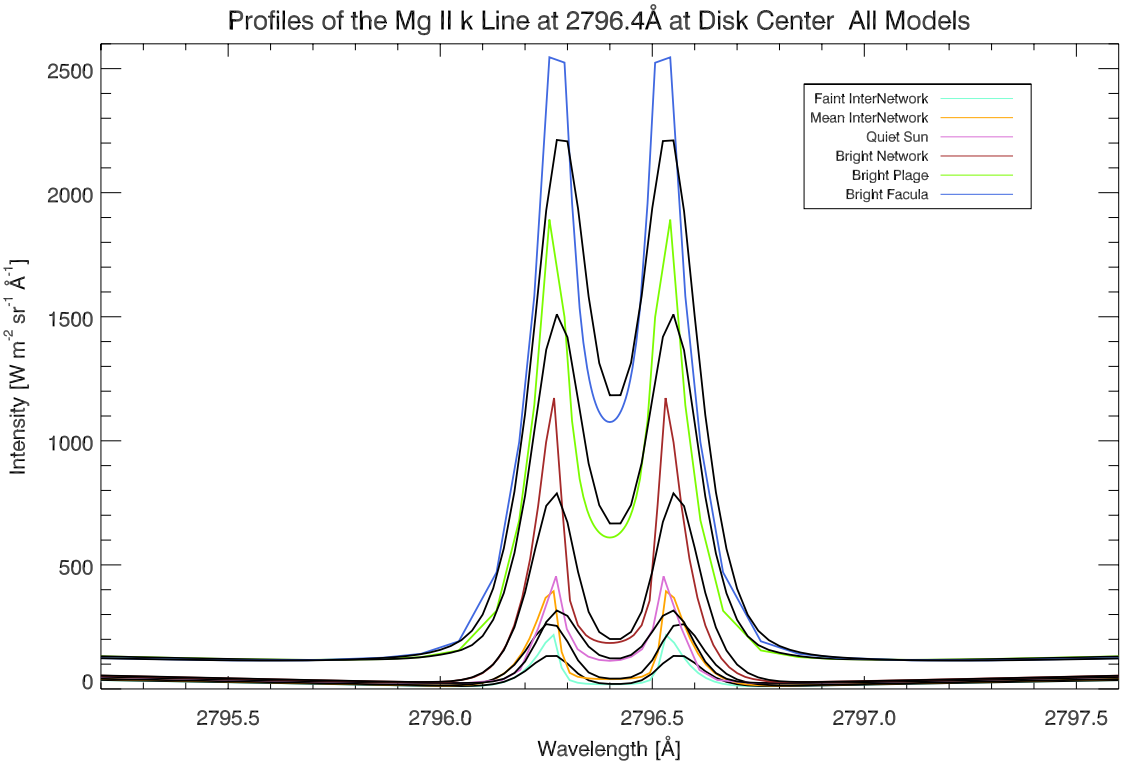

Fig. 1.— Profiles of the Mg II k line at 2796.4 A at disk center for each of the brightness-component models and the average quiet-Sun model. The profiles shown in color are the calculated ones, and the corresponding ones in black have been convolved with a Gaussian instrumental profile having a FWHM of 80 mÅ, representing the expected IRIS resolution.

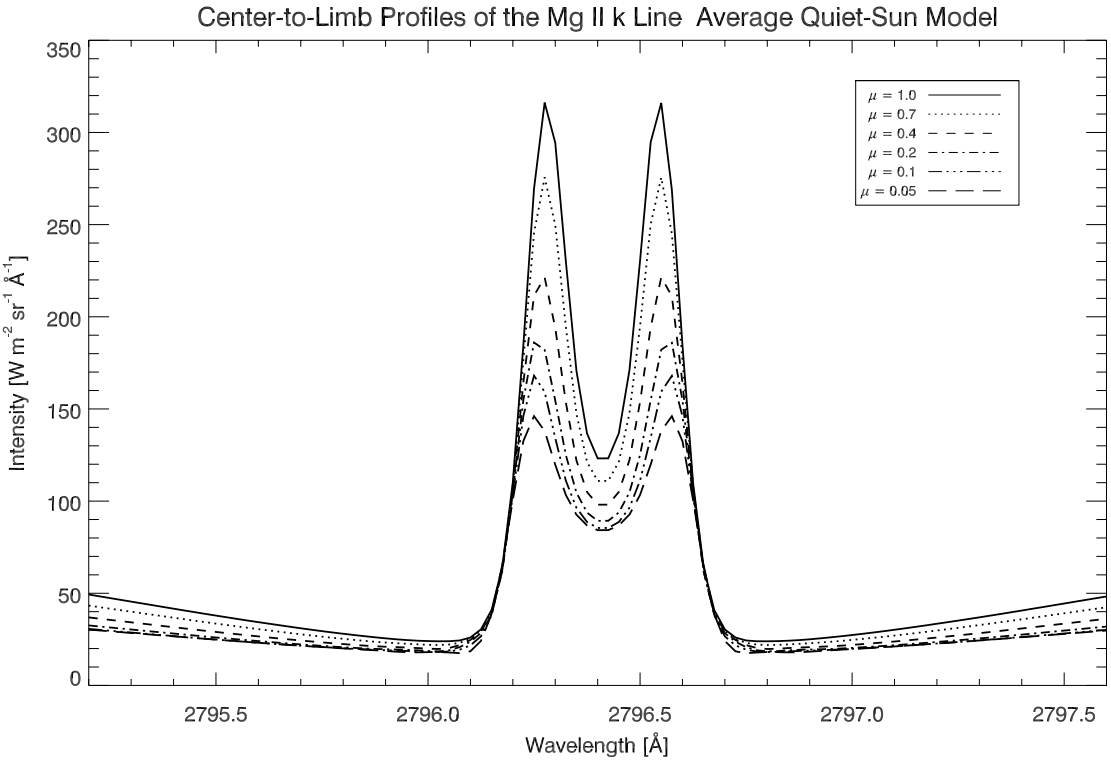

Fig. 2.— Center-to-limb profiles of the Mg II k line calculated from the average quiet-Sun model. Convolved profiles are shown, as in Fig. 1.

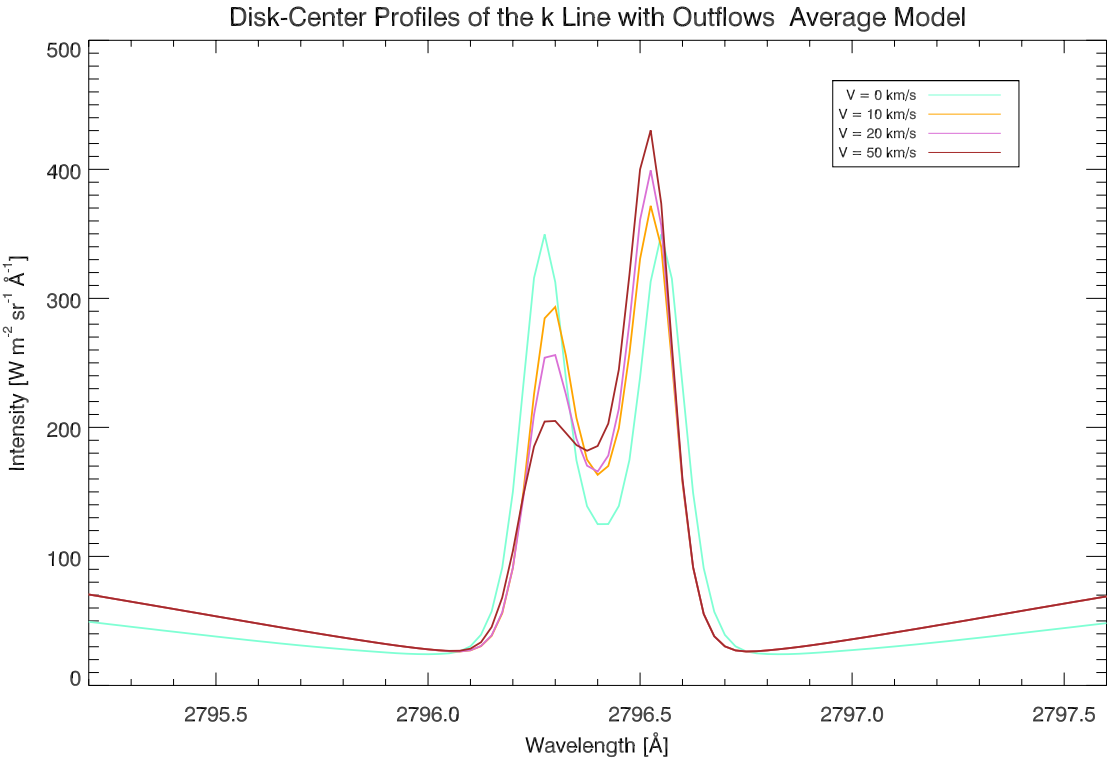

Fig. 3.— Disk-center profiles of the Mg II k line with outflows, calculated from the average quiet-Sun model. Convolved profiles are shown, as in Fig. 1.

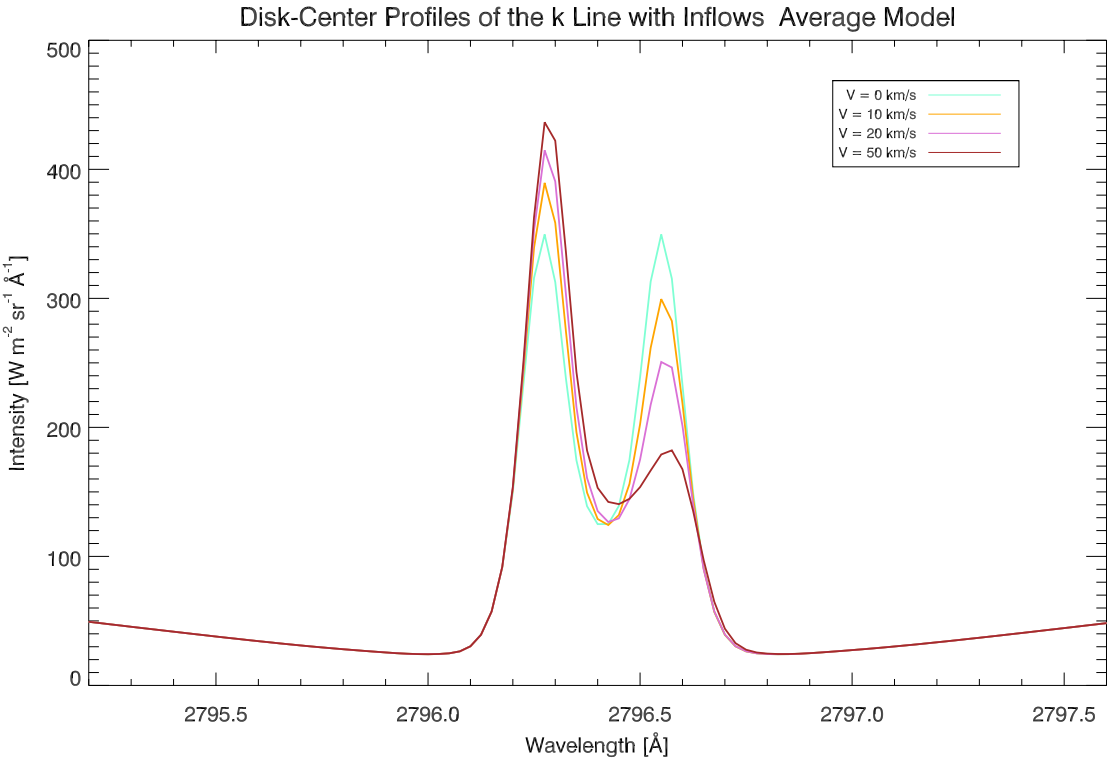

Fig. 4.— Disk-center profiles of the Mg II k line with inflows, calculated from the average quiet-Sun model. Convolved profiles are shown, as in Fig. 1.